



# Dietary inulin decreases circulating ceramides by suppressing neutral sphingomyelinase expression and activity in mice<sup>S</sup>

Pan Deng,<sup>\*,†</sup> Jessie B. Hoffman,<sup>\*,§</sup> Michael C. Petriello,<sup>\*,\*\*\*</sup> Chun-Yan Wang,<sup>\*,†</sup> Xu-Sheng Li,<sup>\*,††</sup> Maria P. Kraemer,<sup>\*\*</sup> Andrew J. Morris,<sup>\*\*\*</sup> and Bernhard Hennig<sup>1,\*,†</sup>

Superfund Research Center,<sup>\*</sup> Department of Animal and Food Sciences, College of Agriculture, Food, and Environment,<sup>†</sup> Department of Pharmacology and Nutritional Sciences,<sup>§</sup> Division of Cardiovascular Medicine, College of Medicine and Lexington Veterans Affairs Medical Center,<sup>\*\*</sup> University of Kentucky, Lexington, KY 40536; and Department of Food Science and Engineering,<sup>††</sup> Jinan University, Guangzhou, China 510632

ORCID ID: 0000-0003-2974-7389 (P.D.)

**Abstract** Elevated circulating levels of ceramides (Cers) are associated with increased risk of cardiometabolic diseases, and Cers may play a causative role in metabolic dysfunction that precedes cardiac events, such as mortality as a result of coronary artery disease. Although the mechanisms involved are likely complex, these associations suggest that lowering circulating Cer levels could be protective against cardiovascular diseases. Conversely, dietary fibers, such as inulin, have been reported to promote cardiovascular and metabolic health. However, the mechanisms involved in these protective processes also are not well understood. We studied the effects of inulin on lipid metabolism with a model of atherosclerosis in LDL receptor-deficient mice using lipidomics and transcriptomics. Plasma and tissues were collected at 10 days and/or 12 weeks after feeding mice an atherogenic diet supplemented with inulin or cellulose (control). Compared with controls, inulin-fed mice displayed a decreased C16:0/C24:0 plasma Cer ratio and lower levels of circulating Cers associated with VLDL and LDL. Liver transcriptomic analysis revealed that *Smpd3*, a gene that encodes neutral SMase (NSMase), was downregulated by 2-fold in inulin-fed mice. Hepatic NSMase activity was 3-fold lower in inulin-fed mice than in controls. Furthermore, liver redox status and compositions of phosphatidylserine and FFA species, the major factors that determine NSMase activity, were also modified by inulin.<sup>¶¶</sup> Taken together, these results showed that, in mice, inulin can decrease plasma Cer levels through reductions in NSMase expression and activity, suggesting a mechanism by which fiber could reduce cardiometabolic disease risk.—Deng, P., J. B. Hoffman, M. C. Petriello, C.-Y. Wang, X.-S. Li, M. P. Kraemer, A. J. Morris, and B. Hennig.

**Dietary inulin decreases circulating ceramides by suppressing neutral sphingomyelinase expression and activity in mice.** *J. Lipid Res.* 2020. 60: 45–53.

**Supplementary key words** fiber • lipidomics • transcriptomics

Soluble fibers such as inulin-type fructans are natural components of several edible fruits and vegetables, and the average individual daily consumption has been estimated to be between 1 and 11 g in Europe and the United States (1, 2). A very recent meta-analysis found that people consuming high levels of dietary fiber have a lower risk of cardiovascular mortality and incidence of common non-communicable diseases, including coronary heart disease and type 2 diabetes, than those eating less fiber (3). Dietary supplementation with inulin-type fructans has been associated with the reduction of cardiovascular disease risk in clinical trials (4, 5). Accumulating evidence has revealed that dietary inulin can modulate gut microbiota composition and generate short-chain FAs, which are associated with beneficial effects on host lipid metabolism, such as decreased circulating cholesterol and triglyceride (TG) levels (6–8). However, the effects of inulin on systemic lipid metabolism remain to be investigated. Identification of these mechanisms might lead to improved approaches for dietary interventions to reduce cardiovascular disease risk.

This study was supported in part by the National Institutes of Health/National Institute of Environmental Health Sciences Grant P42ES007380 and National Institutes of Health/National Institute of General Medical Sciences Grants IS10OD021753 and P30 GM127211. The content is solely the responsibility of the authors and does not necessarily represent the official views of the National Institutes of Health. The authors declare that they have no conflicts of interest with the contents of this article.

Manuscript received 16 August 2019 and in revised form 9 October 2019.

Published, *JLR Papers in Press*, October 11, 2019  
DOI <https://doi.org/10.1194/jlr.RA119000346>

Abbreviations: Cer, ceramide; ChE, cholesterol ester; CL, cardiolipin; DEG, differentially expressed gene; DG, diglyceride; DHCer, dihydroceramide; HexCer, glucosylceramide; *Ldlr*<sup>-/-</sup>, LDL receptor knockout; MG, monoglyceride; NSMase, neutral SMase; PS, phosphatidylserine; *Sgms*, SM synthase; *Smpd*, SM phosphodiesterase; TG, triglyceride; UHPLC, ultra-HPLC.

<sup>1</sup>To whom correspondence should be addressed.

e-mail: bhennig@uky.edu

<sup>S</sup> The online version of this article (available at <http://www.jlr.org>) contains a supplement.

Ceramides (Cers) are amide-linked FA esters of sphingosine. They are precursors of complex sphingolipids. Both *in vitro* and *in vivo* studies have shown that the aberrant accumulation of Cer leads to the activation of several signaling systems that induce insulin resistance, hepatic steatosis, and cardiometabolic disorders (9–12), suggesting that Cer plays a causative role in the metabolic dysfunction that precedes cardiovascular events. Recently, several studies reported divergent associations of distinct plasma Cers with cardiovascular disease mortality in patients with coronary artery disease (13–15). Plasma Cer species are prospective biomarkers of adverse cardiovascular events with tests now being offered by the Mayo Clinic (16). Cer can be produced by three different pathways: 1) *de novo* synthesis from palmitate and serine in four sequential reactions in the endoplasmic reticulum; 2) hydrolysis of SM catalyzed by SMase; and 3) a salvage pathway in which sphingosine can be re-esterified to form Cer. Pharmacological inhibition or genetic ablation of enzymes driving Cer synthesis ameliorates atherosclerosis, insulin resistance, and cardiomyopathy (17–21). Although there are no pharmacological strategies that safely and effectively manipulate Cer in humans, dietary interventions via the Mediterranean diet (22) and Nordic diet (23), which contain high levels of dietary fiber, are associated with reductions in plasma Cer levels. Additionally, a fruit and vegetable diet-based intervention designed according to the USDA MyPlate guidelines was shown to be effective at reducing plasma Cer (24). However, the mechanism(s) responsible for these dietary effects remains unclear.

Systems biology is central to the biological and medical sciences (25). The advent of genotyping arrays enabled studies of global transcriptome. Metabolomic/lipidomic analysis, as the last step in a series of changes following external stimuli insult or in pathological states, can directly reveal phenotypic changes of metabolites in living systems. LC-MS-based metabolomic/lipidomic approaches can rapidly and sensitively detect metabolic changes. In the present study, the effects of inulin on lipid metabolism were elucidated in LDL receptor knockout (*Ldlr*<sup>-/-</sup>) mice. Using lipidomics and transcriptomics, the present study demonstrates that inulin feeding can decrease circulating Cer, and this is associated with downregulation of neutral SMase (NSMase) expression and activity. These results provide evidence for a mechanism by which dietary fiber reduces cardiovascular risk and disease.

## MATERIALS AND METHODS

### Chemicals

Lipid internal standards including LPC 17:0, PC 18:0-d13, SM 18:1-d9, phosphatidylserine (PS) 17:0, PE 17:0, and cholesterol-d7 were purchased from Avanti Polar Lipids (Alabaster, AL). Cer 24:1-d7 was obtained from Cayman Chemical (Ann Arbor, MI). Other chemicals and solvents were of reagent grade, except for the HPLC-grade solvents used for LC-MS analysis.

### Animal experiments

Seven-week-old male *Ldlr*<sup>-/-</sup> mice were purchased from Jackson Laboratories (Bar Harbor, ME) and allowed to acclimate for 1 week. All animal studies were performed in accordance with protocols approved by the Institutional Animal Care and Use Committee of University of Kentucky. Efforts were made to minimize the suffering of experimental animals. Animals were housed in plastic cages with corncob bedding, five mice per cage, in an environmentally controlled mouse room. All mice received diets and tap water *ad libitum* throughout the experiment. Mice were randomly divided into study groups (*n* = 10 per group) with half of them receiving the atherogenic Clinton/Cybulsky diet containing 8% cellulose (Research Diets, New Brunswick, NJ; product number D01061401C) and the other half receiving the atherogenic Clinton/Cybulsky diet containing 8% inulin. The *Ldlr*<sup>-/-</sup> mouse model has been previously shown to develop hyperlipidemia after feeding on the base atherogenic diet (26). The content of fiber in diet was chosen to represent a recommended human high fiber consumption that would confer health benefits (3). Further details of the animal diet are described elsewhere (J. Hoffman et al., unpublished observations). After 10 days of feeding, blood was collected from mouse tail veins into tubes containing ethylenediaminetetraacetic acid, and plasma was separated after centrifugation at 3,000 *g* for 15 min at 4°C. At the completion of week 12, animals were anesthetized using isoflurane prior to euthanasia. Plasma samples were harvested and frozen in liquid nitrogen. Tissues were harvested for mRNA and protein, and all samples were stored at -80°C prior to analysis.

### Lipidomic analysis of plasma and liver

Plasma and liver samples were extracted using a method reported before (27). Briefly, 20 mg of liver tissues were homogenized in 200  $\mu$ l of 0.1% ammonium formate. The homogenate was spiked with internal standard solution and mixed with 1.47 ml of methanol. Then, 5 ml of methyl tertiary-butyl ether were added and the sample was shaken for 1 h at room temperature. Phase separation was induced by adding 1.25 ml of water, and the mixture was centrifuged for 10 min at 3,000 *g* at 4°C. The upper lipid phase was then collected and dried under nitrogen. The lipid residue was dissolved in 400  $\mu$ l of mixed solvent of chloroform and methanol (2:1, v/v). For plasma samples, 20  $\mu$ l of plasma were extracted with 500  $\mu$ l of methyl tertiary-butyl ether twice and the combined extract was processed as above. Lipidomic analysis was performed using an Ultimate 3000 ultra-HPLC (UHPLC) system coupled to a Thermo Q-Exactive Orbitrap mass spectrometer equipped with a heated electrospray ion source (Thermo Scientific). Lipid extracts were separated on a Waters ACQUITY BEH C8 column (2.1  $\times$  50 mm, 1.7  $\mu$ m) with the temperature maintained at 40°C. The flow rate was 250  $\mu$ l/min, and the mobile phases consisted of 60:40 water/acetonitrile (A) and 90:10 isopropanol/acetonitrile (B), both containing 10 mM of ammonium formate and 0.1% formic acid. The samples were eluted with a linear gradient from 32% B to 97% B over 25 min, maintained at 97% B for 4 min, and re-equilibrated with 32% B for 6 min. The sample injection volume was 5  $\mu$ l. The mass spectrometer was operated in positive and negative ionization modes. The full scan and fragment spectra were collected at a resolution of 70,000 and 17,500, respectively. Quality control samples prepared from pooled mouse plasma and liver extracts were used to monitor the overall quality of the lipid extraction and MS analyses. Quality control samples were included in batches of analytical samples during the course of the study. The average coefficient of variation of major lipids detected in the quality control samples was 20%. Data analysis and lipid identification were performed using the software LipidSearch 4.1 (Thermo Fisher). Within a lipid class, MainArea values output by LipidSearch were assigned to

each FA moiety of a given lipid species and summed using Microsoft Excel PivotTable. The peak areas of lipids and internal standards of interest were further analyzed using Thermo Xcalibur 4.0 QuanBrowser. The peak areas for each lipid class were normalized by internal standards. For liver samples, the data was further normalized to tissue weight.

### Plasma fractionation using fast protein LC

Fractionation of plasma into lipoprotein-associated pools was performed as described previously (28). Briefly, plasma samples ( $n = 3$  per group) collected after 12 weeks of feeding were pooled for each group, and 50  $\mu$ l of pooled plasma samples were fractionated by fast protein LC using a calibrated Superose 6 increase column (10/300GL; GE Healthcare) attached to an Agilent 1100 HPLC system. The column was equilibrated and eluted with PBS at a flow rate of 0.5 ml/min. Eluate was collected into a 96 deep-well plate using an Agilent 1200 (G1364B) collector as 21 fractions, which included VLDL, LDL, and HDL. Lipids in plasma fractions were analyzed using UHPLC-Q Exactive MS as described above.

### Transcriptome and bioinformatics analysis of mouse liver

Mouse liver samples were homogenized and total RNA was extracted using the TRIzol reagent (Thermo Fisher Scientific Inc., Waltham, MA). The quality of RNA was assessed using the Agilent 2100 Bioanalyzer system and three samples from each group with a RNA integrity number greater than 8 were used for RNA library construction. The library was sequenced by the BGI Americas (San Jose, CA). Single-end reads of 50 bp read-length were sequenced on the BGISEQ-500RS sequencer. The raw data was filtered to remove reads that are at low quality, containing the sequence of adaptor, and high content of unknown bases. After filtering, the remaining reads were stored as FASTQ format. Quality-filtered sequence reads were mapped to mouse genome reference MM10. Readcount data were then subjected to differential expression analysis using the EBSeq method. Genes with a fold change inulin/control  $\geq 2$  and posterior probability of equal expression  $\leq 0.05$  were considered as differentially expressed genes (DEGs). The DEGs were subjected to GO functional enrichment analysis and Kyoto Encyclopedia of Genes and Genomes (KEGG) analysis using algorithms developed by BGI. The calculated  $P$ -value went through Bonferroni correction, taking a corrected  $P$ -value  $\leq 0.05$  as a threshold.

### Real-time PCR

Total RNA was extracted as described above. cDNA was synthesized from total RNA using the QuantiTect reverse transcription kit (Qiagen, Valencia, CA). PCR was performed on the CFX96 Touch real-time PCR detection system (Bio-Rad, Hercules, CA) using the TaqMan Fast Advanced Master Mix (Thermo Fisher Scientific Inc.). Primer sequences from TaqMan gene expression assays (Thermo Fisher Scientific Inc.) were as follows: SM phosphodiesterase (*Smpd1*) (Mm00488318\_m1); *Smpd2* (Mm01188195\_g1); *Smpd3* (Mm00491359\_m1); SM synthase (*Sgms1*) (Mm00522643\_m1); *Sgms2* (Mm00512327\_m1); and  $\beta$  actin (*Actb*) (Mm02619580\_g1). The levels of mRNA were normalized relative to the amount of *Actb* mRNA, and expression levels in mice fed control diet were set at 1. Gene expression levels were calculated according to the  $2^{-\Delta\Delta Ct}$  method (29).

### Measurement of NSMase activity

Liver tissue was homogenized in 40 vol of buffer containing 25 mM Tris-HCl, 150 mM NaCl, and 1% Triton X-100 (pH 7.4). NSMase activity was determined using the assay kit from Echelon Biosciences (Salt Lake City, UT) following the manufacturer's

instructions. Dithiothreitol at 5 mM was added to the incubation mixture to inhibit any acid SMase activity (30). In this assay, NSMase converts SM substrate to phosphocholine, which is hydrolyzed by alkaline phosphatase and reacted with choline oxidase to generate hydrogen peroxide that is measured colorimetrically at 595 nm. A standard curve of absorbance values of known amounts of choline standards was generated. SMase activity in the samples (nanomoles per minute per milliliter) was calculated from their corresponding absorbance values via the standard curve. The enzyme activity was normalized using protein levels quantified by the bicinchoninic acid assay.

### Statistical analyses

Partial least-squares discriminant analysis of lipidomic data was used to identify initial trends and clusters in data sets and was performed using the Metaboanalyst 4.0 web portal (<https://www.metaboanalyst.ca>). Statistical analyses of RT-qPCR gene expression, enzyme activity, and lipidomic data were performed using the GraphPad Prism version 7.04 for Windows (GraphPad Software Inc., La Jolla, CA). Comparisons between groups were made by unpaired Student's  $t$ -test considering significance at the level of  $P < 0.05$ . Data are expressed as mean  $\pm$  SEM.

## RESULTS

### Lipidomic analysis of plasma after inulin feeding for 10 days and 12 weeks

Lipid extracts of plasma collected 10 days and 12 weeks after initiation of feeding the inulin- or cellulose-enriched (control) diet were analyzed using UHPLC-Q Exactive MS. A total of 768 and 747 lipid species were identified in the plasma obtained after 10 days and 12 weeks of feeding, respectively, with coverage of 13 different lipid subclasses across all samples. A partial least-squares discriminant analysis was performed to identify groups of lipids that contribute to the differential effects of inulin diet on the mouse plasma lipidome. There were clear differences between inulin- and cellulose-fed mice in plasma samples obtained after 10 days but not in those after 12 weeks of feeding (supplemental Fig. S1), indicating considerable variation in the plasma lipid composition at 10 days after treatment, and this variation was blunted at 12 weeks. Further analysis of lipidomic data by unpaired Student  $t$ -test revealed that sphingolipids and glycerolipids were the most significantly changed lipid classes between inulin-fed and control mice (Fig. 1). In plasma samples obtained at 10 days after feeding, the total level of diglyceride (DG), monoglycerides (MGs), SM, and Cer was decreased compared with the control group. In plasma samples collected at 12 weeks, the levels of Cer, cholesterol esters (ChEs), and LPC were significantly lower in inulin-fed mice than control mice. Our further studies therefore focused on investigating possible mechanisms linking dietary inulin supplementation to decreases in plasma Cer. In samples obtained after 10 days of feeding, five major Cer species were present at 39–51% lower levels in inulin-treated mice than those in control mice (Fig. 2A). After 12 weeks of feeding, the major Cer species decreased in inulin-fed mice, including Cer 16:0, 20:0, and 24:1, with levels present at 47% lower than those



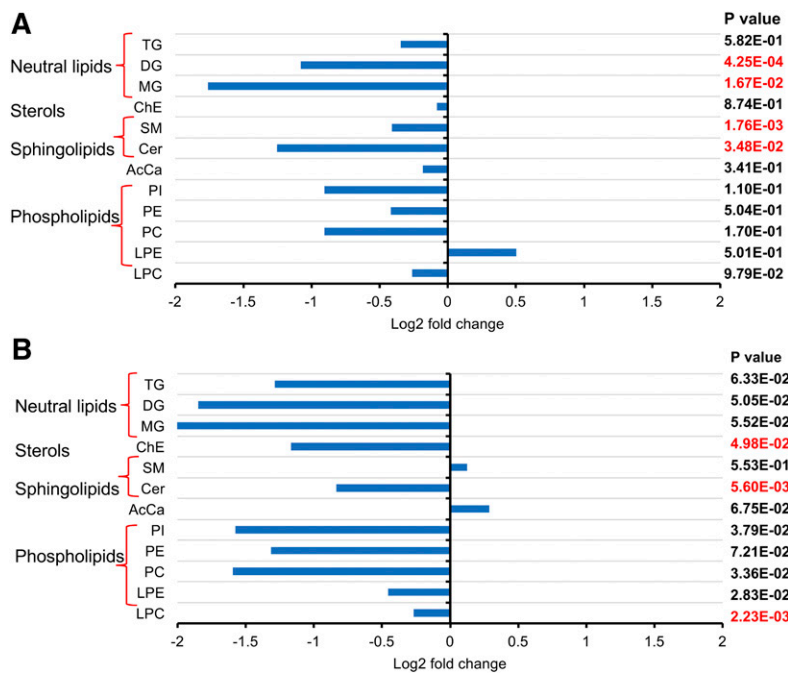


**Fig. 1.** Fold changes of plasma lipids in inulin-fed *Ldlr*<sup>-/-</sup> mice compared with control mice after 10 days (A) and 12 weeks (B) of atherogenic diet feeding (n = 9–10 per group). Lipidomic analysis was performed using UHPLC-Q Exactive MS. Comparisons between groups were made by unpaired Student's *t*-test considering significance at the level of *P* < 0.05. AcCa, acylcarnitine.

in control mice (Fig. 2B). Recent studies have suggested that the ratios between Cer in plasma are more closely related with diseases than the total amounts, particularly the long-chain Cer 16:0, in relation to very-long-chain Cer 24:0 (31). In the present study, the Cer 16:0/C24:0 ratio was calculated and there was no significant difference between the two groups in samples obtained at day 10 after feeding. However, a decreased ratio in the inulin group was observed in samples obtained after 12 weeks of feeding (Fig. 2C). SM is a major precursor for Cer and can be hydrolyzed by SMase to produce Cer. Among the major SM species in plasma, the level of SM 16:0 decreased by 31% after 10 days of inulin treatment (Fig. 3A). After 12 weeks, the levels of SM 20:0 and 22:0 were increased by 74% and 124%, respectively, in inulin-fed mice compared with controls (Fig. 3B). In both 10 day and 12 week plasma samples, ratios of Cer/SM were more than 42% lower in inulin-fed mice than control mice (Fig. 3C, D). Combined, these data suggest that inulin influences the plasma level of sphingolipids, especially Cer, within 10 days after dietary intervention, and the effect persisted for at least 12 weeks.

### Effect of dietary inulin on liver lipidome

Although Cer can be synthesized in virtually every organ, the liver is a key site for Cer production. Additionally, different organs have different Cer profiles, and the Cer composition in plasma is most similar to that in liver

(32). Therefore, mouse liver samples were analyzed using the lipidomic method. Inulin feeding was not associated with significant changes in Cer and SM levels in the liver but significantly altered the contents of DG and cardiolipin (CL) (Fig. 4). CL is an essential phospholipid that makes up to 15–20% of the inner mitochondrial membrane and is linked to mitochondrial function (33, 34). Unlike other hepatic phospholipid classes, which showed no differences after inulin intervention, CL levels were increased by more than 43% in the inulin-fed group, especially CL 72:6, 72:7, 74:9, 74:10, 76:6, 78:11, and 79:9 (supplemental Fig. S2). It was found that, although there were no significant changes in the total levels of PS and FFA (Fig. 4), liver composition of PS and FFA species with various fatty acyl chains were changed after inulin feeding, as demonstrated by no less than 48% increases in levels of PS species with long fatty acyl chains (total carbon number  $\geq 40$ ) and polyunsaturated bonds (double bond number  $\geq 5$ ). On the contrary, PS species with medium fatty acyl chains (total carbon number  $\leq 34$ ) and fewer double bonds (double bond number = 1 or 2) were decreased by more than 34% (Fig. 5A). In all of the 23 FFA species detected in the liver, inulin feeding reduced the levels of 11 unsaturated FAs by 25–51% (Fig. 5B). Taken together, inulin feeding increased liver contents of CL and changed the hepatic compositions of PS and FFA.

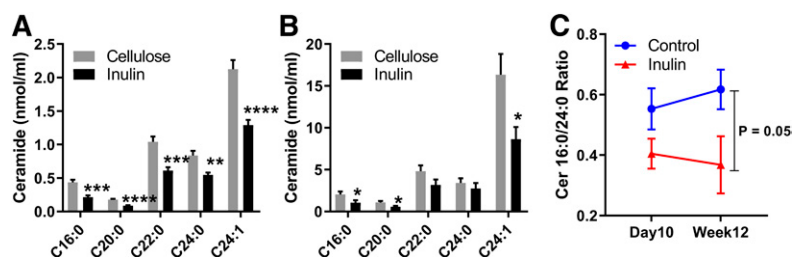


**Fig. 2.** Cer species in the plasma of *Ldlr*<sup>-/-</sup> mice fed an atherogenic diet supplemented with inulin or cellulose (control). After 10 days of feeding (A); after 12 weeks of feeding (B); and the ratios of Cer16:0/24:0 after 10 days and 12 weeks of feeding (C). Cer and SM levels were detected by UHPLC-Q Exactive MS. Mean  $\pm$  SEM is shown (n = 9–10 per group). \*\*\*\**P* < 0.0001, \*\*\**P* < 0.001, \*\**P* < 0.01 (unpaired Student's *t*-test).

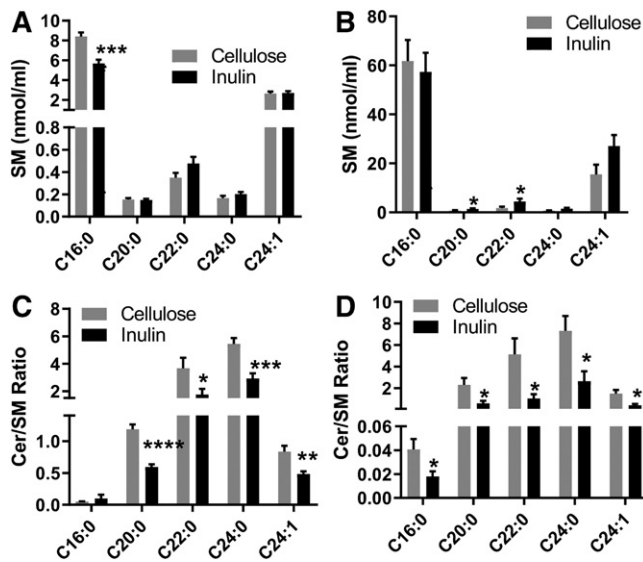


**Fig. 3.** The effects of inulin on plasma SM (A, B) and Cer/SM molar ratio (C, D) in *Ldlr*<sup>-/-</sup> mice. A, C: After 10 days of atherogenic diet feeding. B, D: After 12 weeks of atherogenic diet feeding. Mean  $\pm$  SEM is shown ( $n = 9-10$  per group). \*\*\*\* $P < 0.0001$ , \*\*\* $P < 0.001$ , \*\* $P < 0.01$ , \* $P < 0.05$  (unpaired Student's *t*-test).

### Effect of dietary inulin on lipoprotein-associated sphingolipid levels

Cer is a component of lipoproteins and 98% of plasma Cer is associated with lipoprotein subfractions (35). In control diet-fed mice, Cer was mostly distributed in VLDL and LDL, with less than 14% of Cer associated with HDL (Fig. 6A). Cer with different fatty acyl chains distributed differentially in lipoproteins. Long-chain Cer 16:0 was equally distributed in VLDL (46%) and LDL (40%), whereas more than 60% of very-long-chain Cer 20:0, 22:0, 24:0, and 24:1 was distributed in VLDL, and 17–31% was associated with LDL. In inulin-fed mice, VLDL- and LDL-associated Cer decreased by 4- to 7-fold compared with the control group, and little effect on HDL-Cer was observed in inulin-fed mice compared with controls (Fig. 6A–F), suggesting that dietary inulin decreases VLDL- and LDL- but not HDL-associated Cer. Dihydroceramide (DH-Cer), SM, and glucosylceramide (HexCer) are either precursors or downstream metabolites of Cer. In control diet-fed mice, these sphingolipids demonstrated similar

lipoprotein distributions as Cer with about 50–60% in VLDL, 30% in LDL, and less than 15% in HDL fraction (supplemental Fig. S3). After inulin treatment, the VLDL-associated SM, DHCer, and HexCer were decreased by 1.8- to 5.2-fold compared with controls. There were slight decreases in LDL-associated DHCer and HexCer; however, no obvious changes in HDL-associated DHCer and HexCer were observed. On the contrary, HDL-associated SM was increased by 1.6-fold, and there was no change in LDL-associated SM in inulin-fed mice compared with controls (supplemental Fig. S3).

### Transcriptomic analysis of liver after inulin feeding

To understand the molecular mechanisms underlying the effect of inulin on lipid levels, comparative transcriptomic analysis was performed ( $n = 3$  per group). A total of 59 DEGs were identified in the inulin-fed mice as compared with the control group, with 47 downregulated and 12 upregulated (supplemental Table S1). The DEGs were then subjected to an analysis of their biological functions altered by inulin feeding. As shown in Fig. 7, the top two ranked functions that were modified by inulin were signal transduction and the immune system, and five genes in these two categories related to inflammation, including interleukin-2-inducible T-cell kinase, NLR family apoptosis inhibitory protein 1, plasminogen activator inhibitor 1, C-C motif chemokine ligand 15, and C-C motif chemokine ligand 19, were all downregulated by inulin feeding (supplemental Table S1). These results suggested that inulin may modify the inflammatory process through downregulation of these genes. Furthermore, three genes associated with lipid metabolism were changed due to inulin feeding, including aldo-keto reductase, *Smpd3*, and glutathione peroxidase 6 (*Gpx6*) (supplemental Table S1). *Smpd3* encodes NSMase that catalyzes the hydrolysis of SM to form Cer. Hepatic expression of *Smpd3* was downregulated in inulin-fed mice compared with controls. In order to validate the findings from the transcriptomic analysis, qPCR analysis was performed. Five genes involved in SM-Cer pathways, including *Smpd1*, *Smpd2*, *Smpd3*, *Sgms1*, and *Sgms2*, were examined. We found that the results of qPCR analysis were well matched with the transcriptomic data, with *Smpd3* being the only gene that was downregulated in inulin-fed mouse liver (Fig. 8A).

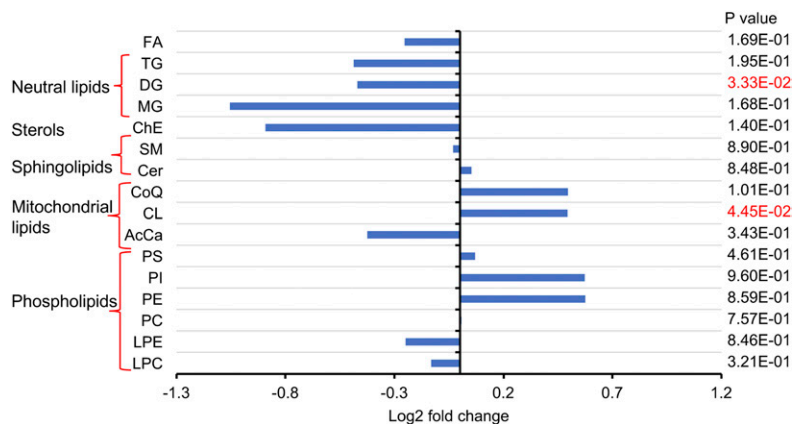


**Fig. 4.** Changes in the liver lipidome of *Ldlr*<sup>-/-</sup> mice after 12 weeks of feeding inulin- or cellulose-supplemented (control) atherogenic diet ( $n = 9-10$  per group). Lipidomic analysis was performed using UH-PLC-Q Exactive MS. Comparisons of total lipid levels between groups were made by unpaired Student's *t*-test considering significance at the level of  $P < 0.05$ . CoQ, coenzyme Q; AcCa, acylcarnitine.

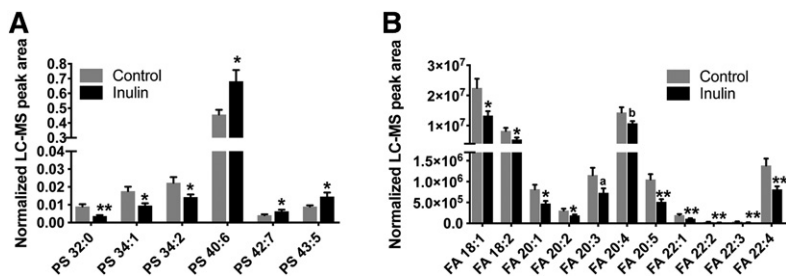


**Fig. 5.** Inulin feeding modifies hepatic composition of PS (A) and FFA (B) in *Ldlr*<sup>-/-</sup> mice. FFA and PS levels were measured by UHPLC-Q Exactive MS as described in the Materials and Methods. Mean  $\pm$  SEM is shown ( $n = 9-10$ ). \*\* $P < 0.01$ , \* $P < 0.05$ ; a $P = 0.06$ , b $P = 0.08$  (unpaired Student's *t*-test).

### Measurement of NSMase enzymatic activity

To investigate the functional relevance of downregulated hepatic gene expression of *Smpd3* in inulin-fed mice, we sought to determine whether inulin feeding leads to changes of NSMase activity in mouse livers. Measurements of catalytic activity revealed that the NSMase activity in inulin-fed mice was reduced by about 4-fold compared with control mice with a *P*-value of 0.005 (Fig. 8B).

### DISCUSSION

Plasma and hepatic lipid (i.e cholesterol and TG) profiles are well understood to change extensively with dietary inulin intervention in humans (8). We used sophisticated lipidomics to analyze the effects of dietary inulin supplementation not only on common and abundant lipids but also on several less abundant lipid classes and species in a well-characterized mouse model. Our study identified Cer as a major circulating lipid class that was downregulated by inulin feeding. Most importantly, the ratio of Cer 16:0/24:0

was decreased in mice after 12 weeks of inulin feeding. Lipoprotein analysis demonstrated that inulin feeding decreased VLDL- and LDL-associated Cer but had little effect on HDL-Cer. We also found that CL is a major lipid class in the liver that differed significantly between the control and inulin groups. Furthermore, hepatic composition of anionic lipids that control NSMase activity were modified due to inulin feeding. This study describes how plasma and hepatic lipid profiles are altered during inulin feeding and highlights the possible implications of these changes on hepatic NSMase activity.

Recent studies revealed that plasma Cer levels correlate strongly with adverse cardiovascular events, and Cers containing the C16:0, C18:0, and C24:1 fatty acyl chains display an independent predictive value of plaque instability and/or future fatality (36). Particularly, high Cer 16:0/24:0 ratios are strongly associated with major adverse cardiac events as well as other metabolic defects, including coronary artery disease and insulin resistance (31). Our results indicated that the short-term (10 days) feeding of inulin could lower plasma levels of Cer but had no effect on the

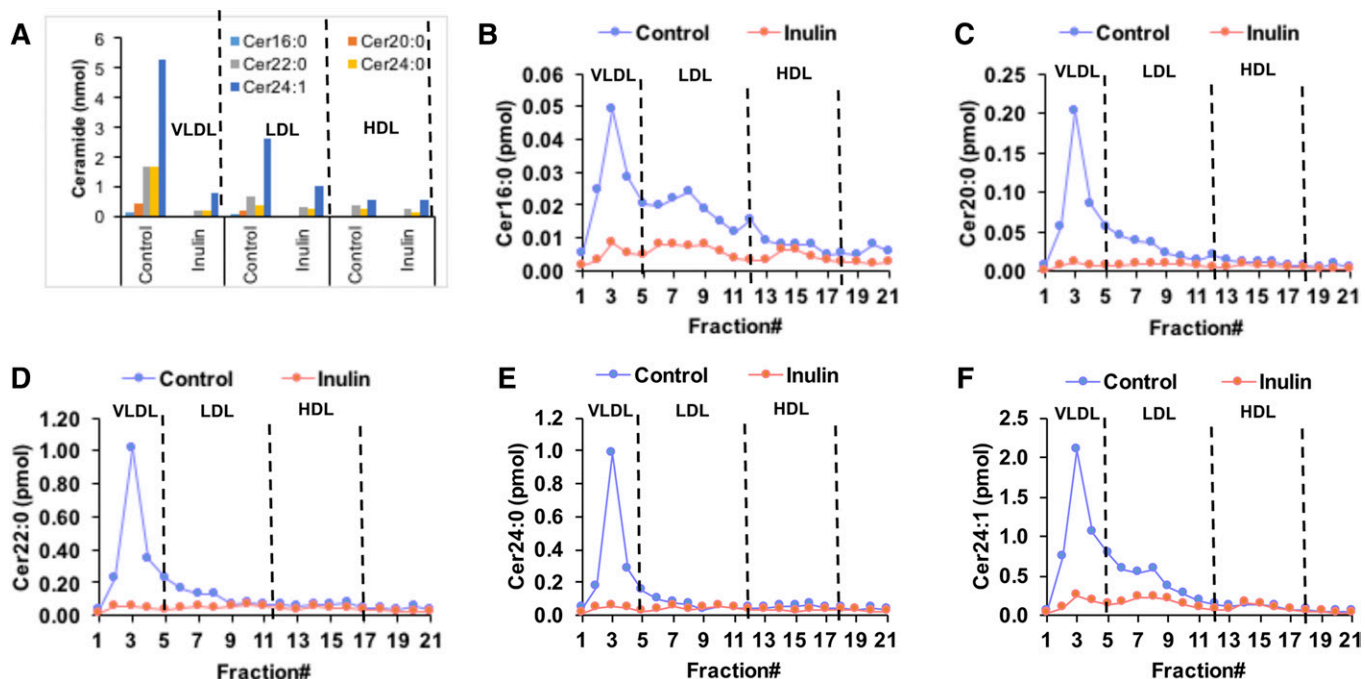


**Fig. 6.** Changes in plasma lipoprotein-associated Cer after 12 weeks of feeding an inulin- or cellulose-supplemented (control) atherogenic diet to *Ldlr*<sup>-/-</sup> mice. Plasma samples from three mice in each group were pooled and lipoproteins including VLDL, LDL, and HDL were fractionated using fast protein LC. Cers in samples were detected by UHPLC-Q Exactive MS. A: Comparison of individual Cer species in the total VLDL-, LDL-, and HDL-associated fractions of inulin and control diet-fed mice. B-F: Levels of individual Cer species present in each fraction obtained from fast protein LC.



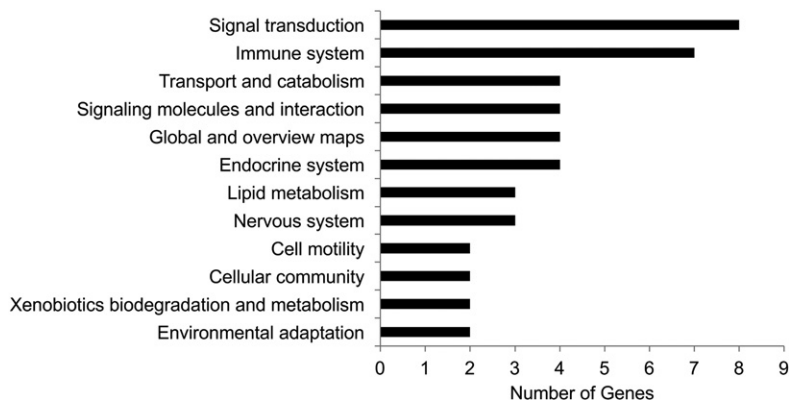


**Fig. 7.** Differential expressed hepatic genes in inulin-fed mice versus control mice. Genes with a fold change inulin/control  $\geq 2$  and posterior probability of equal expression  $\leq 0.05$  were considered as DEGs. The DEGs were subjected to GO functional enrichment analysis. The calculated *P*-value goes through Bonferroni correction. The pathways that have more than two genes enriched are shown. See also supplemental Table S1 for raw data.

ratio of Cer 16:0/24:0. However, after long-term (12 weeks) inulin treatment, not only was the plasma level of Cer lowered but the ratio of Cer 16:0/24:0 was also decreased compared with cellulose-fed control mice. These results suggested a beneficial effect of long-term inulin dietary intervention. Cer can be produced from SM catalyzed by SMases, which are classified based on their pH optima of activity into acid, neutral, and alkaline subtypes, and NSMase appears to be the predominant enzyme involved in cell growth, apoptosis, and inflammation (37, 38). We found that dietary inulin feeding lowered plasma Cer levels in an atherogenic mouse model, and this effect was associated with downregulated *Smpd3* expression and NSMase activity. Previous studies showed that NSMase is activated by unsaturated FA and anionic phospholipids, and specifically by PS (39, 40). In addition, it is a redox-sensitive enzyme with TNF- $\alpha$ , oxidative stress, and inflammation being potent activators and antioxidants like glutathione acting as strong inhibitors (41). In inulin-fed mice, the hepatic levels of polyunsaturated FFAs were significantly reduced compared with control mice, especially linoleic acid (C18:2) (Fig. 5B), which is an established stimulator of NSMase (39). Additionally, although there was no difference in the total level of hepatic PS between inulin and control mice, the PS molecular species were significantly modified by inulin feeding. A decreased level of PS with medium fatty acyl chain lengths (PS 32:0, 34:1, 34:2) and an increased level of PS with long polyunsaturated fatty acyl chains (PS 40:6, 42:7, 43:5) were observed in livers from inulin-fed mice compared with controls (Fig. 5A). Recent structural analysis revealed two binding sites for PS in NSMase (39, 42), which are critical for the activation of NSMase. Therefore,

inulin-induced alterations in FA and PS levels and molecular species composition could potentially contribute to decreased NSMase activity.

It was reported that aggregation-prone human LDL particles were enriched with Cer (43). Additionally, Cer transported in LDL was elevated in the plasma of obese patients with type 2 diabetes and correlated with insulin resistance (35). This suggests that LDL-associated Cer is involved in the progression of cardiometabolic diseases, and reducing Cer packaging into lipoprotein may provide cardiovascular health benefits. In the present study, inulin-fed mice showed decreased levels of Cer in both VLDL and LDL, and this may partially be due to reduction of plasma VLDL particles by dietary inulin as reported previously (44). This is also supported by our observation that VLDL cholesterol (VLDL-C) was decreased in mice fed with inulin for 12 weeks, whereas LDL-C and HDL-C were not significantly affected by diet (supplemental Fig. S4). Additionally, liver lipids, including TG and ChE, both of which are important in VLDL assembly, were depleted by inulin feeding (Fig. 4), and this could subsequently lead to decreased production of VLDL in the liver. It is interesting that, in response to dietary inulin, SM demonstrated a different lipoprotein profile compared with Cer, with more being incorporated into HDL, whereas no significant changes were observed in the LDL (supplemental Fig. S3). An increased level of HDL-SM is an inverse risk factor for coronary heart disease (45); therefore, enhanced incorporation of SM into HDL by inulin could be associated with beneficial health effects. Further studies are warranted to understand the mechanism of how inulin can modify sphingolipid packaging into lipoproteins.

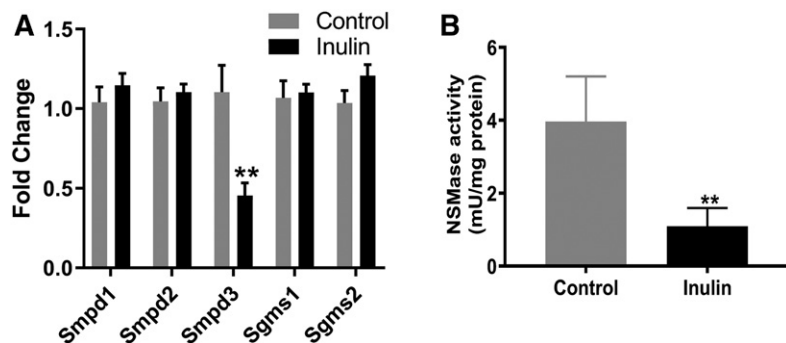



**Fig. 8.** Effects of inulin on *Smpd3* gene expression and NSMase activity in the livers of *Ldlr*<sup>-/-</sup> mice. A: Quantitative PCR was performed to confirm the effects of inulin on sphingolipid metabolism genes. *Smpd3* is the only gene that was downregulated in inulin-fed mice. B: Liver NSMase activity was investigated as described in the Materials and Methods. The bars represent the mean  $\pm$  SEM of four samples in each group. \*\**P* < 0.01 (unpaired Student's *t*-test).

CL is a unique phospholipid almost exclusively located at the level of the inner mitochondrial membrane (46). This phospholipid is known to be intimately involved in several mitochondrial bioenergetic processes. CL is particularly susceptible to reactive oxygen species attack due to its high content of unsaturated FAs (47). In the livers of inulin-fed mice, the levels of CL were significantly higher compared with control mice (Fig. 4, supplemental Fig. S2). Transcriptomics analysis demonstrated that several hepatic genes related to inflammation were downregulated (Fig. 7); among these were plasminogen activator inhibitor 1 and C-C motif chemokine ligand 5, which are known to be positively related to redox status (48, 49). We hypothesized that the increased CL observed in inulin-fed mice was indicative of enhanced mitochondrial function, which may be augmented by inulin feeding to maintain redox homeostasis in response to oxidative stress in this atherogenic mouse model. Because NSMase is a redox-sensitive enzyme (37), the effect of inulin on redox balance may also contribute to the lower NSMase activity observed in inulin-fed mice.

It is interesting that although inulin feeding decreased plasma levels of Cer (Fig. 2), it did not alter Cer or SM contents in the liver (Fig. 4) and intestine (data not shown), two major organs for Cer biosynthesis. Similar observations were reported in studies using an NSMase inhibitor, GW4869 (50–52). Systemic administration of GW4869 to mice did not alter the Cer or SM content in the liver but did decrease circulating Cer levels (50–52). This might be because Cer flux between the liver and plasma was decreased by NSMase inhibition without changing steady state levels in the liver. Cer could be generated through three pathways, including de novo synthesis from long-chain FAs, the SMase-catalyzed hydrolysis of SM, and via the salvage pathway. Our lipidomics analysis of liver samples revealed that the contents of DHCer species were increased in inulin-fed mice (supplemental Fig. S4), and this partially supported our hypothesis that de novo synthesis is a compensatory pathway for Cer synthesis after SMase is inhibited; therefore, the steady state levels of Cer in liver could be maintained.

Inulin-type fructans have been demonstrated to improve cardiovascular health through a number of mechanisms, including modifying de novo lipid synthesis, increasing muscle lipoprotein lipase enzyme activity, enhancing the production of short-chain FAs, increasing the fecal excretion of bile salts and cholesterol (7, 53), and reversing endothelial dysfunction via activation of the nitric oxide synthase pathway (8). Our study identified a novel mechanism by which dietary inulin alters sphingolipid metabolism through downregulation of NSMase activity and thereby decreasing circulating Cer levels. Additionally, we observed that VLDL cholesterol was decreased in mice fed with inulin for 12 weeks, and LDL-C and HDL-C were not significantly affected (supplemental Fig. S5), which was consistent with data reported by Trautwein, Rieckhoff, and Erberdobler (44). Furthermore, sphingolipid profiles in VLDL and LDL were significantly modified in inulin-fed mice compared with the control group (Fig. 6). Those results indicated that inulin could potentially change lipoprotein compositions and functions, but how this will

contribute to the anti-atherogenic effects of inulin is largely unknown. A long-term study is warranted to further explore the impacts of inulin on lipoproteins, Cer, and the pathology of atherosclerosis.

In summary, we demonstrated that, in an atherogenic mouse model, inulin feeding decreased plasma levels of Cer within 10 days, and this effect persisted to at least 12 weeks. Lipoprotein analysis indicated that inulin decreased VLDL- and LDL-associated Cer. Transcriptomics and qPCR revealed that inulin feeding downregulated hepatic *Smpd3* expression. NSMase activity was lower in inulin-fed mice compared with the controls. In addition to decreased expression this could partially be due to decreases in NSMase activation of anionic lipids (PS and FFA) and perhaps also to suppression of oxidative stress in the liver. These findings suggest that dietary fiber might be an effective way to reduce plasma Cer in humans, which could have beneficial effects on the cardiovascular risks and metabolic diseases that have been associated with elevated circulating Cer levels. 

## REFERENCES

- van Loo, J., P. Coussement, L. de Leenheer, H. Hoebregs, and G. Smits. 1995. On the presence of inulin and oligofructose as natural ingredients in the Western diet. *Crit. Rev. Food Sci. Nutr.* **35**: 525–552.
- Moshfegh, A. J., J. E. Friday, J. P. Goldman, and J. K. Ahuja. 1999. Presence of inulin and oligofructose in the diets of Americans. *J. Nutr.* **129**: 1407S–1411S.
- Reynolds, A., J. Mann, J. Cummings, N. Winter, E. Mete, and L. Te Morenga. 2019. Carbohydrate quality and human health: a series of systematic reviews and meta-analyses. *Lancet.* **393**: 434–445.
- Beylot, M. 2005. Effects of inulin-type fructans on lipid metabolism in man and in animal models. *Br. J. Nutr.* **93**(Suppl 1): S163–S168.
- Liu, F., M. Prabhakar, J. Ju, H. Long, and H. W. Zhou. 2017. Effect of inulin-type fructans on blood lipid profile and glucose level: a systematic review and meta-analysis of randomized controlled trials. *Eur. J. Clin. Nutr.* **71**: 9–20.
- Everard, A., V. Lazarevic, M. Derrien, M. Girard, G. G. Muccioli, A. M. Neyrinck, S. Possemiers, A. Van Holle, P. Francois, W. M. de Vos, et al. 2011. Responses of gut microbiota and glucose and lipid metabolism to prebiotics in genetic obese and diet-induced leptin-resistant mice. *Diabetes.* **60**: 2775–2786. [Erratum. 2011. *Diabetes.* **60**: 3307.]
- Singh, A., R. C. Zapata, A. Pezeshki, R. D. Reidelberger, and P. K. Chelikani. 2018. Inulin fiber dose-dependently modulates energy balance, glucose tolerance, gut microbiota, hormones and diet preference in high-fat-fed male rats. *J. Nutr. Biochem.* **59**: 142–152.
- Reis, S. A., L. L. Conceicao, D. D. Rosa, M. M. Dias, and C. Peluzio Mdo. 2014. Mechanisms used by inulin-type fructans to improve the lipid profile. *Nutr. Hosp.* **31**: 528–534.
- Summers, S. A. 2006. Ceramides in insulin resistance and lipotoxicity. *Prog. Lipid Res.* **45**: 42–72.
- Holland, W. L., and S. A. Summers. 2008. Sphingolipids, insulin resistance, and metabolic disease: new insights from in vivo manipulation of sphingolipid metabolism. *Endocr. Rev.* **29**: 381–402.
- Summers, S. A. 2015. The ART of Lowering Ceramides. *Cell Metab.* **22**: 195–196.
- Chaurasia, B., and S. A. Summers. 2015. Ceramides - lipotoxic inducers of metabolic disorders. *Trends Endocrinol. Metab.* **26**: 538–550.
- Laaksonen, R., K. Ekroos, M. Sysi-Aho, M. Hilvo, T. Vihervaara, D. Kauhanen, M. Suoniemi, R. Hurme, W. Marz, H. Scharnagl, et al. 2016. Plasma ceramides predict cardiovascular death in patients with stable coronary artery disease and acute coronary syndromes beyond LDL-cholesterol. *Eur. Heart J.* **37**: 1967–1976.
- Tarasov, K., K. Ekroos, M. Suoniemi, D. Kauhanen, T. Sylvanne, R. Hurme, I. Gouni-Berthold, H. K. Berthold, M. E. Kleber, R. Laaksonen, et al. 2014. Molecular lipids identify cardiovascular risk and are efficiently lowered by simvastatin and PCSK9 deficiency. *J. Clin. Endocrinol. Metab.* **99**: E45–E52.



15. de Carvalho, L. P., S. H. Tan, G. S. Ow, Z. Tang, J. Ching, J. P. Kovalik, S. C. Poh, C. T. Chin, A. M. Richards, E. C. Martinez, et al. 2018. Plasma ceramides as prognostic biomarkers and their arterial and myocardial tissue correlates in acute myocardial infarction. *JACC Basic Transl. Sci.* **3**: 163–175.
16. Nicholls, M. 2017. Plasma ceramides and cardiac risk. *Eur. Heart J.* **38**: 1359–1360.
17. Bikman, B. T., Y. Guan, G. Shui, M. M. Siddique, W. L. Holland, J. Y. Kim, G. Fabrias, M. R. Wenk, and S. A. Summers. 2012. Fenretinide prevents lipid-induced insulin resistance by blocking ceramide biosynthesis. *J. Biol. Chem.* **287**: 17426–17437.
18. Hojjati, M. R., Z. Li, H. Zhou, S. Tang, C. Huan, E. Ooi, S. Lu, and X. C. Jiang. 2005. Effect of myriocin on plasma sphingolipid metabolism and atherosclerosis in apoE-deficient mice. *J. Biol. Chem.* **280**: 10284–10289.
19. Chaurasia, B., V. A. Kaddai, G. I. Lancaster, D. C. Henstridge, S. Sriram, D. L. Galam, V. Gopalan, K. N. Prakash, S. S. Velan, S. Bulchand, et al. 2016. Adipocyte ceramides regulate subcutaneous adipose browning, inflammation, and metabolism. *Cell Metab.* **24**: 820–834.
20. Zhang, Q. J., W. L. Holland, L. Wilson, J. M. Tanner, D. Kearns, J. M. Cahoon, D. Pettey, J. Losee, B. Duncan, D. Gale, et al. 2012. Ceramide mediates vascular dysfunction in diet-induced obesity by PP2A-mediated dephosphorylation of the eNOS-Akt complex. *Diabetes.* **61**: 1848–1859.
21. Siddique, M. M., Y. Li, L. Wang, J. Ching, M. Mal, O. Ilkayeva, Y. J. Wu, B. H. Bay, and S. A. Summers. 2013. Ablation of dihydroceramide desaturase 1, a therapeutic target for the treatment of metabolic diseases, simultaneously stimulates anabolic and catabolic signaling. *Mol. Cell. Biol.* **33**: 2353–2369.
22. Wang, D. D., E. Toledo, A. Hruby, B. A. Rosner, W. C. Willett, Q. Sun, C. Razquin, Y. Zheng, M. Ruiz-Canela, M. Guasch-Ferre, et al. 2017. Plasma ceramides, Mediterranean diet, and incident cardiovascular disease in the PREDIMED trial (Prevention con Dieta Mediterranea). *Circulation.* **135**: 2028–2040.
23. Lankinen, M., U. Schwab, M. Kolehmainen, J. Paananen, H. Nygren, T. Seppanen-Laakso, K. Poutanen, T. Hyotylainen, U. Riserus, M. J. Savolainen, et al. 2016. A healthy Nordic diet alters the plasma lipidomic profile in adults with features of metabolic syndrome in a multicenter randomized dietary intervention. *J. Nutr.* **146**: 662–672.
24. Mathews, A. T., O. A. Famodu, M. D. Olfert, P. J. Murray, C. F. Cuff, M. T. Downes, N. J. Haughey, S. E. Colby, P. D. Chantler, I. M. Olfert, et al. 2017. Efficacy of nutritional interventions to lower circulating ceramides in young adults: FRUVEDomic pilot study. *Physiol. Rep.* **5**: e13329.
25. Yan, J., S. L. Risacher, L. Shen, and A. J. Saykin. 2018. Network approaches to systems biology analysis of complex disease: integrative methods for multi-omics data. *Brief. Bioinform.* **19**: 1370–1381.
26. Teupser, D., A. D. Persky, and J. L. Breslow. 2003. Induction of atherosclerosis by low-fat, semisynthetic diets in LDL receptor-deficient C57BL/6J and FVB/NJ mice: comparison of lesions of the aortic root, brachiocephalic artery, and whole aorta (en face measurement). *Arterioscler. Thromb. Vasc. Biol.* **23**: 1907–1913.
27. Matyash, V., G. Liebisch, T. V. Kurzchalia, A. Shevchenko, and D. Schwudke. 2008. Lipid extraction by methyl-tert-butyl ether for high-throughput lipidomics. *J. Lipid Res.* **49**: 1137–1146.
28. Walton, R. G., B. Zhu, R. Unal, M. Spencer, M. Sunkara, A. J. Morris, R. Charnigo, W. S. Katz, A. Daugherty, D. A. Howatt, et al. 2015. Increasing adipocyte lipoprotein lipase improves glucose metabolism in high fat diet-induced obesity. *J. Biol. Chem.* **290**: 11547–11556.
29. Livak, K. J., and T. D. Schmittgen. 2001. Analysis of relative gene expression data using real-time quantitative PCR and the 2<sup>(-Delta Delta C(T))</sup> method. *Methods.* **25**: 402–408.
30. Qin, J., E. Berdyshev, C. Poirer, N. B. Schwartz, and G. Dawson. 2012. Neutral sphingomyelinase 2 deficiency increases hyaluronan synthesis by up-regulation of hyaluronan synthase 2 through decreased ceramide production and activation of Akt. *J. Biol. Chem.* **287**: 13620–13632.
31. Tippetts, T. S., W. L. Holland, and S. A. Summers. 2018. The ceramide ratio: a predictor of cardiometabolic risk. *J. Lipid Res.* **59**: 1549–1550.
32. Schiffmann, S., K. Birod, J. Mannich, M. Eberle, M. S. Wegner, R. Wanger, D. Hartmann, N. Ferreiros, G. Geisslinger, and S. Grosch. 2013. Ceramide metabolism in mouse tissue. *Int. J. Biochem. Cell Biol.* **45**: 1886–1894.
33. Chicco, A. J., and G. C. Sparagna. 2007. Role of cardiolipin alterations in mitochondrial dysfunction and disease. *Am. J. Physiol. Cell Physiol.* **292**: C33–C44.
34. Wang, Y., and S. Hekimi. 2016. Understanding ubiquinone. *Trends Cell Biol.* **26**: 367–378.
35. Boon, J., A. J. Hoy, R. Stark, R. D. Brown, R. C. Meex, D. C. Henstridge, S. Schenk, P. J. Meikle, J. F. Horowitz, B. A. Kingwell, et al. 2013. Ceramides contained in LDL are elevated in type 2 diabetes and promote inflammation and skeletal muscle insulin resistance. *Diabetes.* **62**: 401–410.
36. Summers, S. A. 2018. Could ceramides become the new cholesterol? *Cell Metab.* **27**: 276–280.
37. Shamseddine, A. A., M. V. Airola, and Y. A. Hannun. 2015. Roles and regulation of neutral sphingomyelinase-2 in cellular and pathological processes. *Adv. Biol. Regul.* **57**: 24–41.
38. Clarke, C. J., and Y. A. Hannun. 2006. Neutral sphingomyelinases and nSMase2: bridging the gaps. *Biochim. Biophys. Acta.* **1758**: 1893–1901.
39. Hofmann, K., S. Tomiuk, G. Wolff, and W. Stoffel. 2000. Cloning and characterization of the mammalian brain-specific, Mg<sup>2+</sup>-dependent neutral sphingomyelinase. *Proc. Natl. Acad. Sci. USA.* **97**: 5895–5900.
40. Liu, B., D. F. Hassler, G. K. Smith, K. Weaver, and Y. A. Hannun. 1998. Purification and characterization of a membrane bound neutral pH optimum magnesium-dependent and phosphatidylserine-stimulated sphingomyelinase from rat brain. *J. Biol. Chem.* **273**: 34472–34479.
41. Dotson 2nd, P. P., A. A. Karakashian, and M. N. Nikolova-Karakashian. 2015. Neutral sphingomyelinase-2 is a redox sensitive enzyme: role of catalytic cysteine residues in regulation of enzymatic activity through changes in oligomeric state. *Biochem. J.* **465**: 371–382.
42. Airola, M. V., P. Shanbhogue, A. A. Shamseddine, K. E. Guja, C. E. Senkal, R. Maini, N. Bartke, B. X. Wu, L. M. Obeid, M. Garcia-Diaz, et al. 2017. Structure of human nSMase2 reveals an interdomain allosteric activation mechanism for ceramide generation. *Proc. Natl. Acad. Sci. USA.* **114**: E5549–E5558.
43. Ruuth, M., S. D. Nguyen, T. Vihervaara, M. Hilvo, T. D. Laajala, P. K. Kondadi, A. Gistera, H. Lahteenmaki, T. Kittila, J. Huusko, et al. 2018. Susceptibility of low-density lipoprotein particles to aggregate depends on particle lipidome, is modifiable, and associates with future cardiovascular deaths. *Eur. Heart J.* **39**: 2562–2573.
44. Trautwein, E. A., D. Rieckhoff, and H. F. Erbersdobler. 1998. Dietary inulin lowers plasma cholesterol and triacylglycerol and alters biliary bile acid profile in hamsters. *J. Nutr.* **128**: 1937–1943.
45. Martínez-Beamonte, R., J. M. Lou-Bonafonte, M. V. Martínez-Gracia, and J. Osada. 2013. Sphingomyelin in high-density lipoproteins: structural role and biological function. *Int. J. Mol. Sci.* **14**: 7716–7741.
46. Kim, J., P. E. Minkler, R. G. Salomon, V. E. Anderson, and C. L. Hoppel. 2011. Cardiolipin: characterization of distinct oxidized molecular species. *J. Lipid Res.* **52**: 125–135.
47. Dudek, J. 2017. Role of cardiolipin in mitochondrial signaling pathways. *Front. Cell Dev. Biol.* **5**: 90.
48. Liu, R. M. 2008. Oxidative stress, plasminogen activator inhibitor 1, and lung fibrosis. *Antioxid. Redox Signal.* **10**: 303–319.
49. Qiu, L., L. Ding, J. Huang, D. Wang, J. Zhang, and B. Guo. 2009. Induction of copper/zinc-superoxide dismutase by CCL5/CCR5 activation causes tumour necrosis factor-alpha and reactive oxygen species production in macrophages. *Immunology.* **128**: e325–e334.
50. Tabatadze, N., A. Savonenko, H. Song, V. V. Bandaru, M. Chu, and N. J. Haughey. 2010. Inhibition of neutral sphingomyelinase-2 perturbs brain sphingolipid balance and spatial memory in mice. *J. Neurosci. Res.* **88**: 2940–2951.
51. Lallemand, T., M. Rouahi, A. Swiader, M. H. Grazide, N. Geoffre, P. Alayrac, E. Reczens, A. Coste, R. Salvayre, A. Negre-Salvayre, et al. 2018. nSMase2 (type 2-neutral sphingomyelinase) deficiency or inhibition by GW4869 reduces inflammation and atherosclerosis in ApoE(-/-) mice. *Arterioscler. Thromb. Vasc. Biol.* **38**: 1479–1492.
52. Unal, B., F. Ozcan, H. Tuzcu, E. Kirac, G. O. Elpek, and M. Aslan. 2017. Inhibition of neutral sphingomyelinase decreases elevated levels of nitrate and oxidative stress markers in liver ischemia-reperfusion injury. *Redox Rep.* **22**: 147–159.
53. Caty, E., L. B. Bindels, A. Tailleux, S. Lestavel, A. M. Neyrinck, J. F. Goossens, I. Lobysheva, H. Plovier, A. Essaghir, J. B. Demoulin, et al. 2018. Targeting the gut microbiota with inulin-type fructans: preclinical demonstration of a novel approach in the management of endothelial dysfunction. *Gut.* **67**: 271–283.